2nd International Accelerator School for Linear Colliders, Erice, Sicily

1 – 10 October, 2007

Damping Rings

Lecture 4

Technical Subsystems

Andy Wolski

University of Liverpool and the Cockcroft Institute

Contents

Lecture 4: Technical Subsystems

The objectives of this lecture are to discuss some of the specifications for and issues with important technical subsystems in the damping rings, in particular, for:

- the injection and extraction kickers;
- the damping wiggler;
- the vacuum system;
- the instrumentation and diagnostics.

Two of the main effects of concern for the vacuum system are electron cloud and ion instabilities. We shall discuss these effects in some detail.

Injection/extraction kickers

The injection/extraction kickers must be capable of injecting and extracting individual bunches in the damping rings.

The requirements are for:

- sufficiently large voltage pulse to provide the necessary deflection angle;
- voltage pulse turning on and off in the 3 ns gap between bunches;
- good pulse-to-pulse stability to avoid trajectory jitter in the deflected bunches;
- good reliability operating at 6 MHz burst repetition rate for 1 ms pulses.

Decompressing the bunch train from the damping rings to the main linac

To make the damping rings practicable, we must "compress" the bunch train.

To decompress the bunch train going into the main linac, we extract bunches one at a time from the damping rings, using a fast (~ 3 ns rise/fall time) kicker.

Consider a damping ring with h stored bunches, with bunch separation Δt. If we fire the extraction kicker to extract every n^{th} bunch, where n is *not* a factor of h, then we extract a continuous train of h bunches, with bunch spacing $n \times \Delta t$.

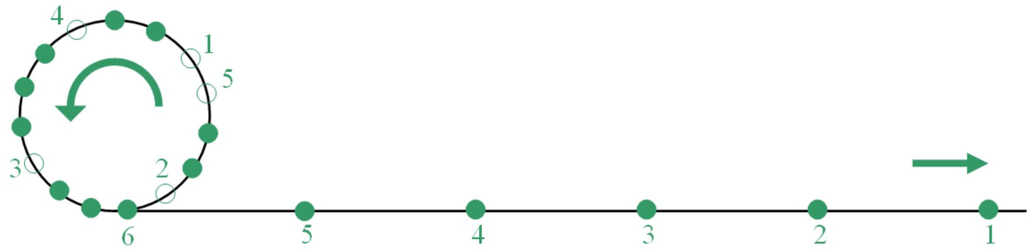

There are two complications:

- We would like a continuous train of bunches in the linac, but the damping rings need to have regular gaps in the fill, for ion clearing.
- The positrons are produced by the decompressed electron beam, so we have no control over the arrival of positron bunches to refill the damping ring. This places a constraint on beam line lengths in the ILC.

Kickers provide a deflecting field to direct incoming bunches onto the orbit

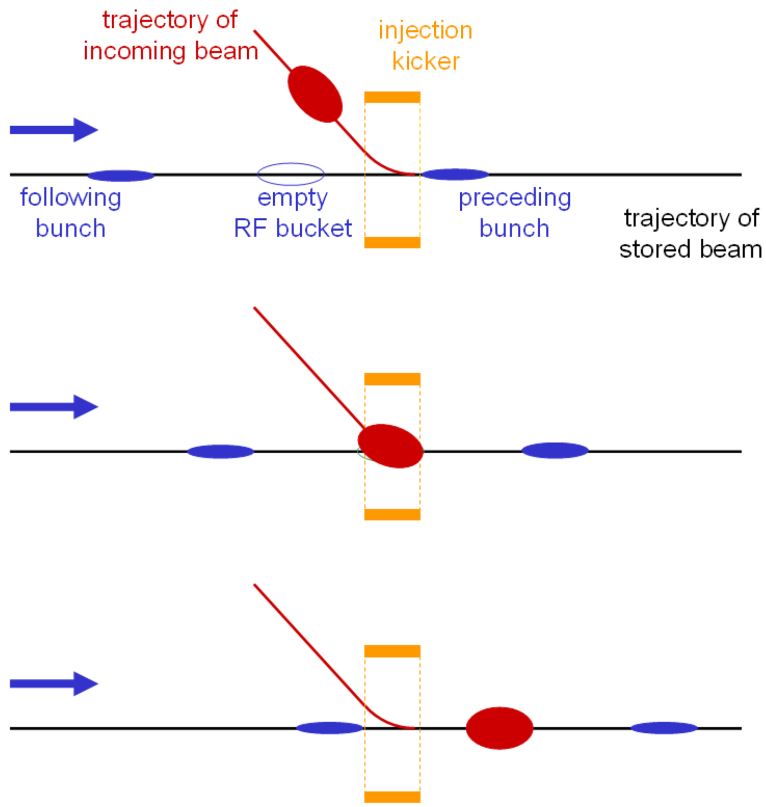

1. Kicker is OFF. "Preceding" bunch exits kicker electrodes. Kicker starts to turn ON.
2. Kicker is ON. "Incoming" bunch is deflected by kicker. Kicker starts to turn OFF.
3. Kicker is OFF by the time the following bunch reaches the kicker.

Injection and extraction kickers

In the ILC damping rings, we need to inject and extract bunches individually, without affecting bunches

Several different types of fast kicker are possible. For the ILC damping rings, the injection/extraction kickers are composed of two parts:

- fast, high-power pulser, that generates a nanosecond voltage pulse;
- stripline electrodes that "deliver" a deflecting field to the beam.

Several technologies are possible for the fast, high-power pulser. The parameters for the ILC damping rings are very challenging, and pulser development is on-going.

The stripline electrodes are conceptually straightforward: they consist of two plates, connected to a high-voltage line, between which the beam travels.

For the ILC damping rings, the stripline design is fairly challenging, because of the need to provide a large on-axis field while maintaining field quality and physical aperture; and the need to match the impedance to the power supply.

Example: stripline electrodes for DAΦNE

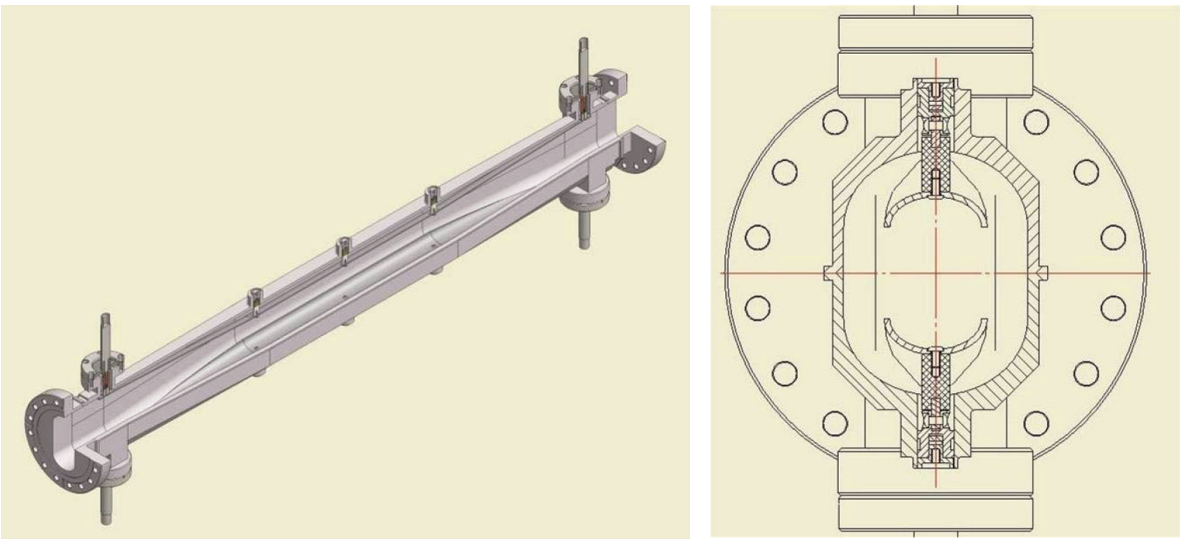

Stripline electrodes developed for fast kicker in DAΦNE.

(D. Alesini, F. Marcellini, P. Raimondi, S. Guiducci, "Fast kickers R&D at LNF-INFN", presented at ILCDR06)

Injection and extraction kickers: a simplified model

Let us take a simplified model of the stripline electrodes, consisting of two infinite parallel plates. The beam travels in the $+z$ direction. We apply an alternating voltage between the plates:

$$V = V_0 e^{i\omega t}$$

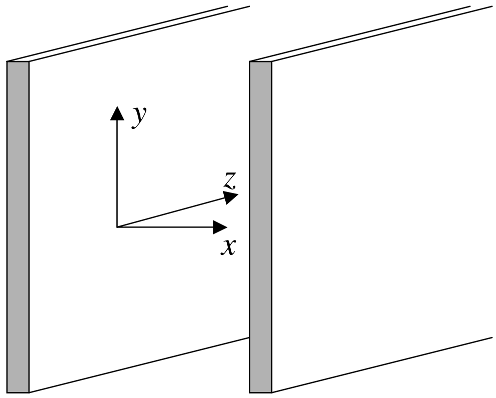

From Maxwell's equations, there are electric and magnetic fields between the plates:

$$E_x = E_0 e^{i(kz-\omega t)} \qquad B_y = \frac{E_0}{c} e^{i(kz-\omega t)}$$

A particle traveling in the $+z$ direction with speed βc will experience a force:

$$F_x = q\left(E_x - v_z B_y\right) = q(1-\beta)E_0 e^{-i(1-\beta)\omega t}$$

For an ultra-relativistic particle, $\beta \approx 1$, and the electric and magnetic forces almost exactly cancel: the resultant force is small. But for a particle traveling in the opposite direction to the electromagnetic wave, $\beta \approx -1$, and the resultant force is twice as large as would be expected from the electric force alone.

Injection and extraction kickers: a simplified model

Let us calculate the deflection of a particle traveling between a pair of stripline electrodes. Let us suppose that there is a voltage pulse of amplitude V and length $2L$ traveling along the electrodes, which consist of infinitely wide parallel plates of length L separated by a distance d:

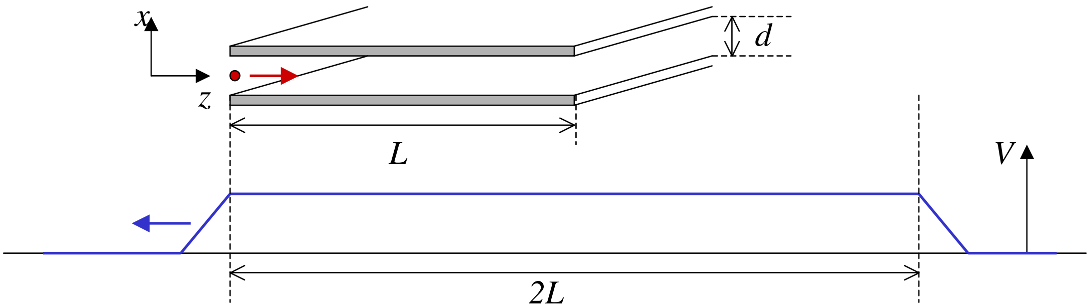

The change in the (normalised) horizontal momentum of the particle is:

$$\Delta p_x = \frac{F_x}{p_0}\frac{L}{c} = 2\frac{V}{E/e}\frac{L}{d}$$

where E is the beam energy. In practice, we can account for the fact that the electrodes are not infinite parallel plates by including a geometry factor, g.

Injection and extraction kickers: a simplified model

How large a kick is needed? Consider the extraction optics:

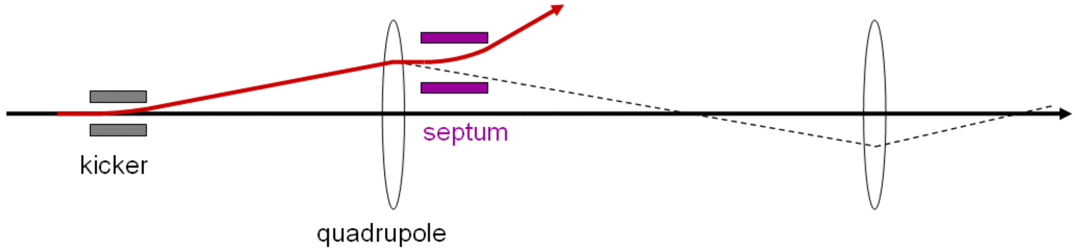

Assuming a distance from the kicker to the septum of 50 m, and a required beam offset from the reference trajectory of 30 mm at the septum, the necessary kick is:

$$\Delta p_x = 2g\frac{V}{E/e}\frac{L}{d} = \frac{0.03}{50} = 0.6\ \mathrm{mrad}$$

If we assume $E/e = 5$ GV, $L = 30$ cm, $d = 20$ mm and $g = 0.7$, we find that the required voltage pulse is 143 kV. This is not realistic for a ~ ns pulser! The solution is to use multiple pairs of striplines, each producing a ~ 10 kV kick.

The length of the stripline adds to the effective rise and fall time

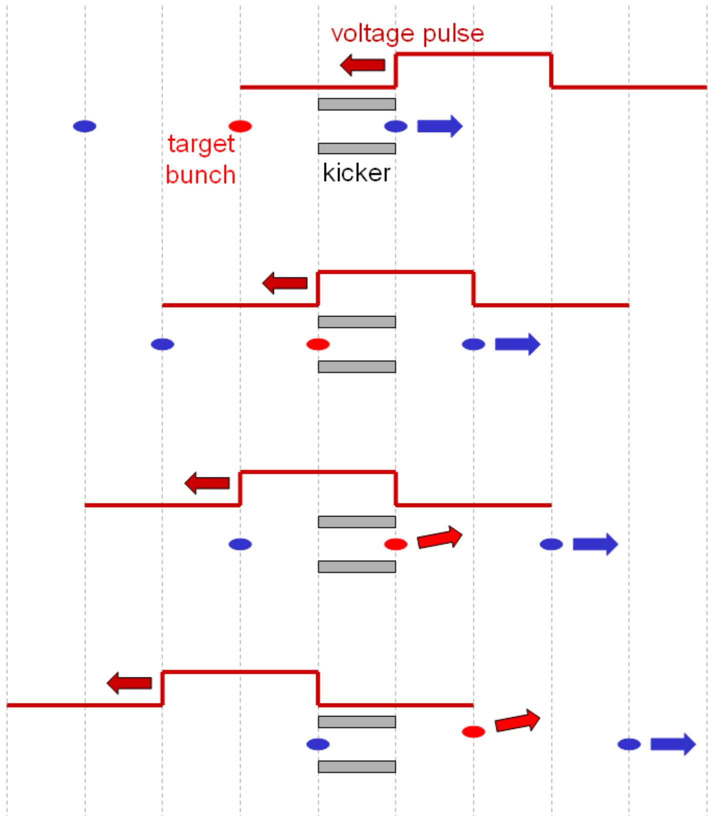

Stage 1: Leading bunch must exit kicker before voltage pulse arrives.

Stage 2: Voltage pulse fills kicker as target bunch arrives.

Stage 3: Voltage pulse continues to fill kicker while target bunch is between striplines.

Stage 4: Voltage pulse exits kicker before trailing bunch arrives.

ILC damping rings fast kicker pulser parameters

The pulsers for the damping rings injection/extraction kickers must meet very demanding specifications:

- peak voltage 10 kV
- rise and fall times ~ 1 ns
- flat-top 2 ns
- "burst" repetition rate 6 MHz
- "burst" pulse length 1 ms
- pulse-to-pulse amplitude stability better than 0.1%

Development of a technology to meet these specifications is the goal of an active R&D program.

Several approaches look promising…

High voltage pulsers for fast kickers: drift step recovery diode (DSRD)

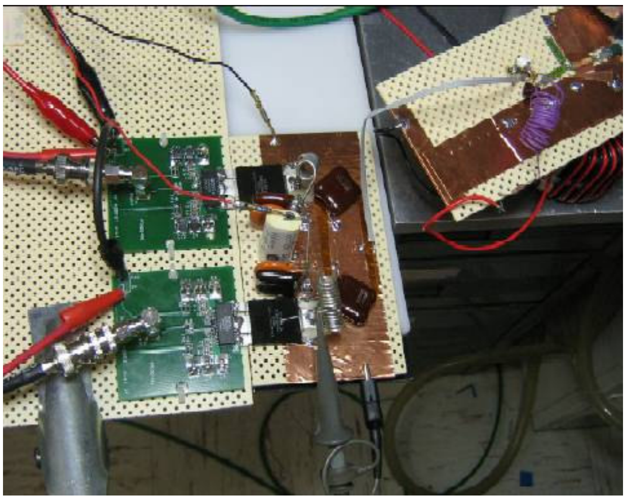

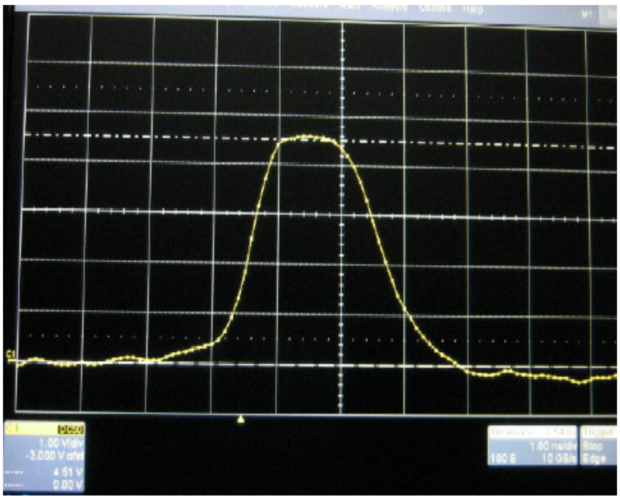

Tests of DSRD fast pulser. Output voltage 2.7 kV; horizontal scale 1 ns/division. (Anatoly Krasnykh)

High voltage pulsers for fast kickers: inductive adder

Output connectors

Trigger cables

Housing for trigger distribution, power supplies, etc.

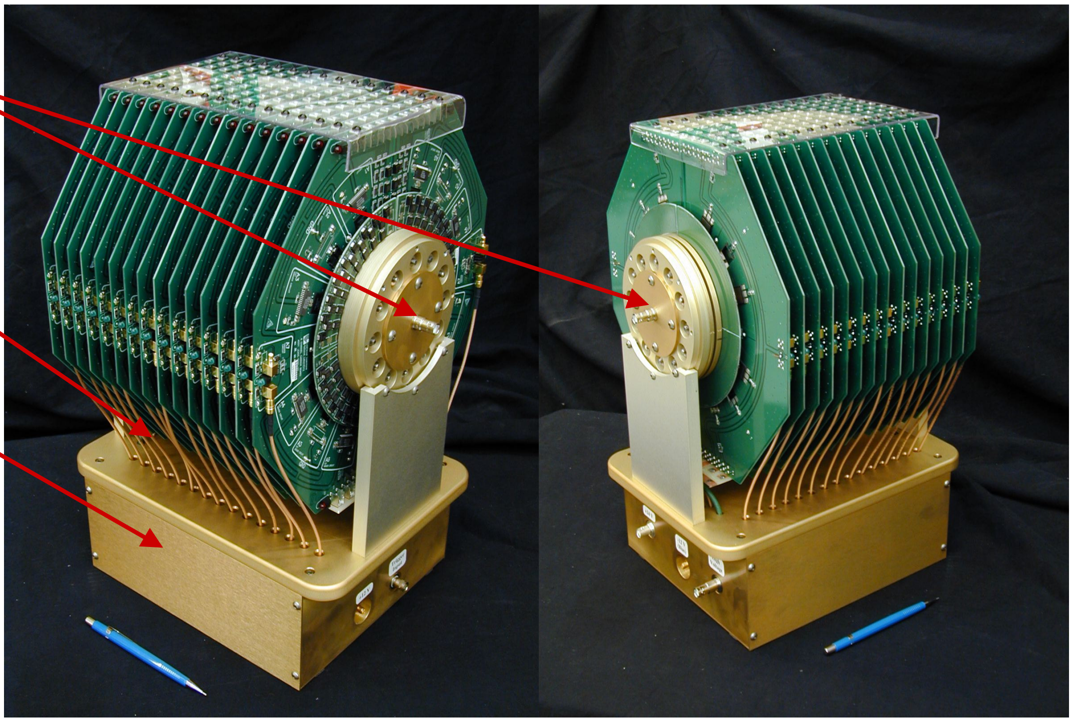

Prototype inductive adder for tests at KEK-ATF. (Ed Cook)

High voltage pulsers for fast kickers: inductive adder

7 ns rise/fall times demonstrated in bench tests of prototype inductive adder. (Ed Cook)

Simultaneous bi-polar outputs: 50 Ω load on each end.

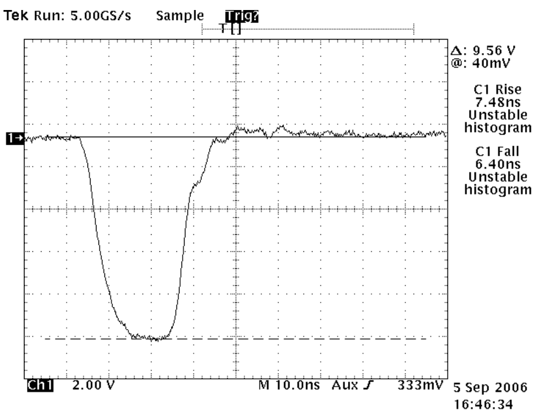

Negative output:
-9.6 kV flat-top

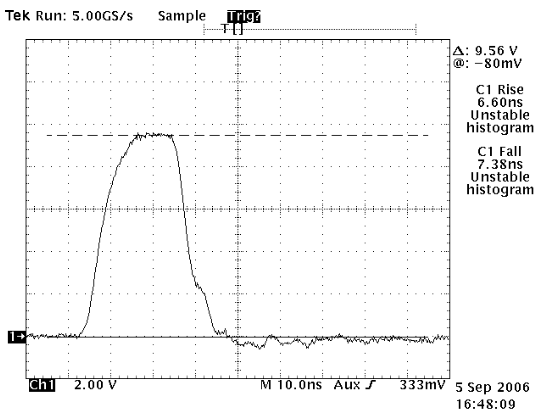

Positive output:
+9.6 kV flat-top

High voltage pulsers for fast kickers: fast ionization dynistor (FID)

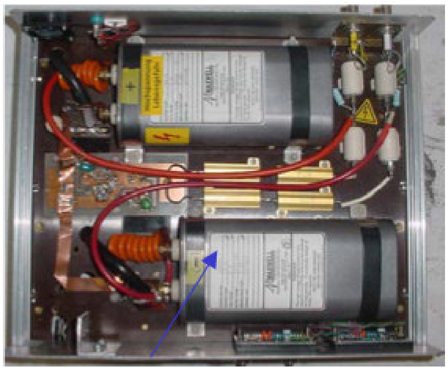

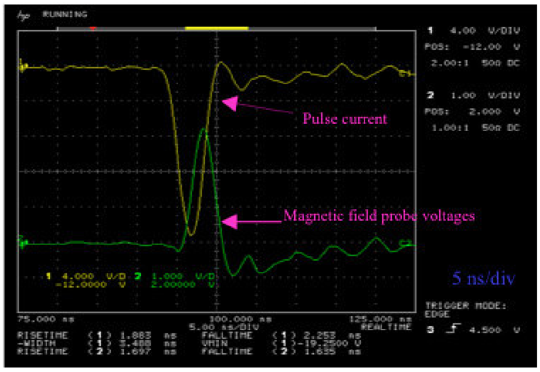

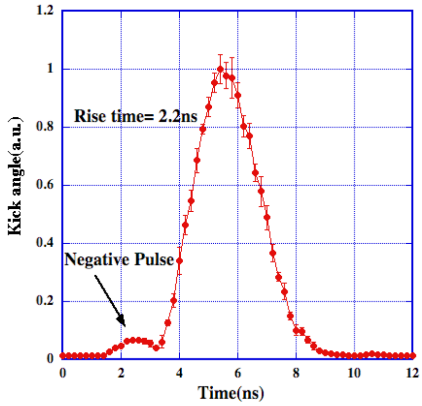

Tests of FID fast pulser at KEK-ATF.
(T. Naito)

Damping wigglers

The damping wigglers are needed to enhance the synchrotron radiation energy losses from particles in the damping rings, hence reducing the radiation damping times.

The wigglers must:

- meet the specifications for field strength and wiggler period set by beam dynamics considerations;
- have reasonable construction and operating costs;
- have a large physical aperture, to ensure good injection efficiency for the positron beam;
- have a good field quality, to avoid adverse impact on the dynamic aperture of the lattice;
- operate reliably over the operating life of the ILC, in a high radiation environment.

Different technology options are available…

A normal-conducting electromagnetic wiggler (from KEK-ATF)

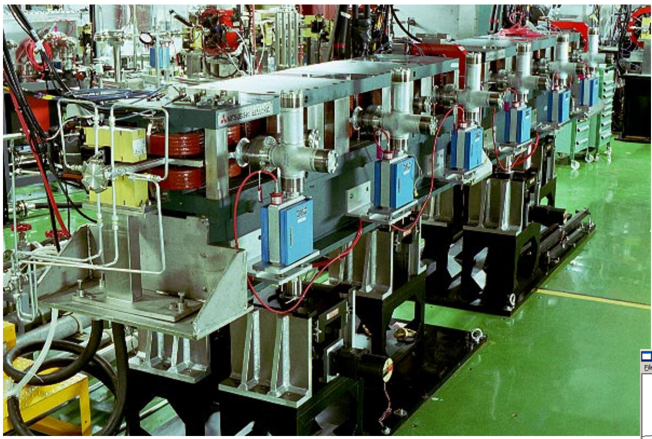

Advantages:

- Conventional, established technology.
- Relatively low construction costs.
- Resistant to radiation damage.
- Good reliability.

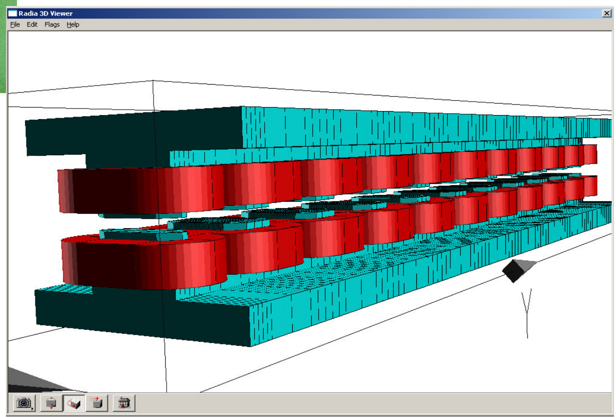

Drawbacks:

- Limited aperture at high field strength.
- High running costs for ILC (~ $1M/year).

Hybrid (permanent magnet and iron) wiggler

Advantages:

- No power consumption.
- No auxiliary systems (cryogenics).

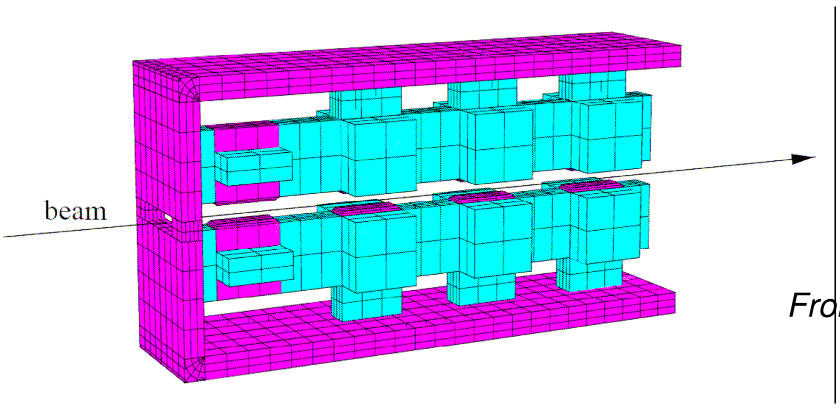

From TESLA TDR

Drawbacks:

- Large amounts of permanent magnet material required to achieve field strength and good field quality at wide aperture – high construction costs.
- Sensitive to radiation (beam losses) – causes loss in field strength, or activation of permanent magnet material.

A superconducting wiggler (from CESR-c)

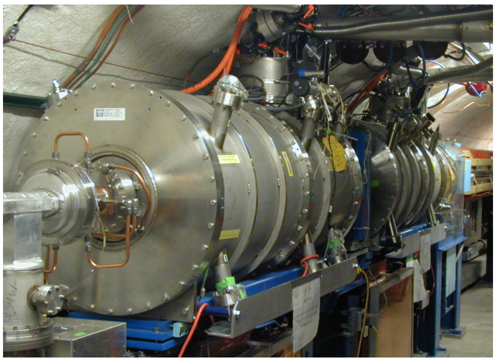

Advantages:

- Large physical aperture.
- Good field quality.
- CESR-c wigglers provide good prototype for ILC damping rings.

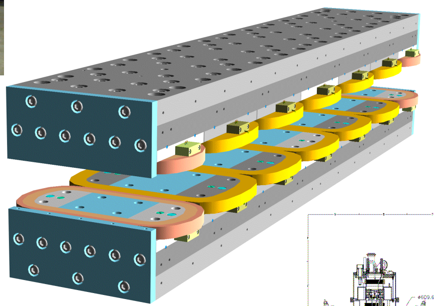

Drawbacks:

- Higher construction costs than for normal conducting wiggler.
- Potentially sensitive to radiation (beam losses).
- Requires auxiliary systems (power supply and cryogenics).

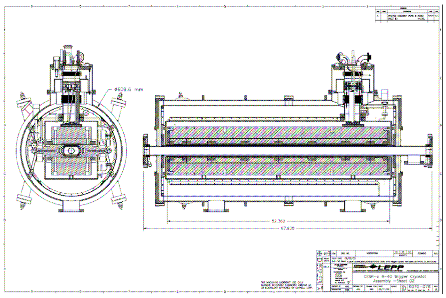

Horizontal focusing in a wiggler

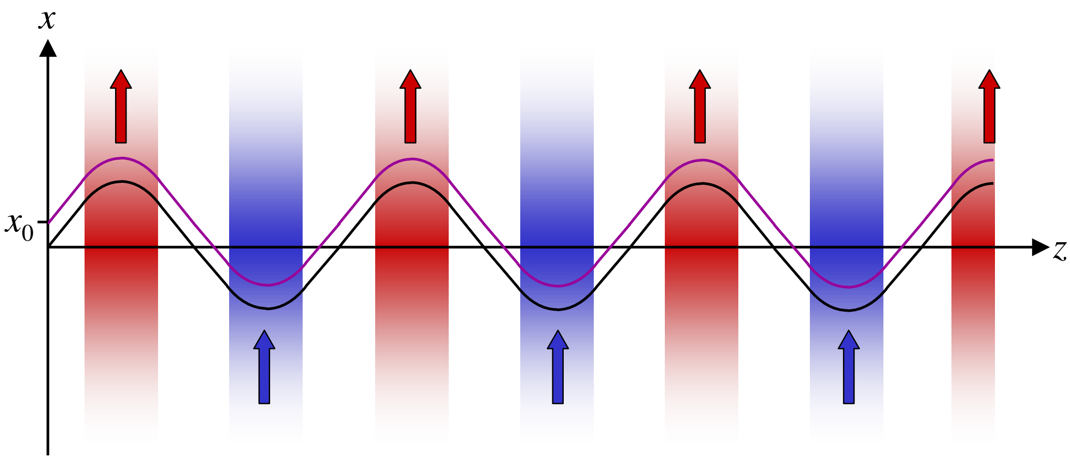

The roll-off in the wiggler field means that a particle with non-zero initial horizontal coordinate sees alternately weaker and stronger fields in successive poles.

The net effect is a horizontal deflection that appears as a horizontal defocusing force: this needs to be properly modelled and accounted for in the lattice design.

Effects of nonlinear wiggler fields

The magnetic fields in a wiggler are intrinsically nonlinear.

Nonlinearities in the magnetic fields in a storage ring can destabilise the betatron oscillations at sufficiently large amplitude: the range of stable amplitudes is known as the "dynamic aperture" of the lattice.

The nonlinearities in the field of the wiggler must be sufficiently small as not to cause an unacceptable limitation in dynamic aperture.

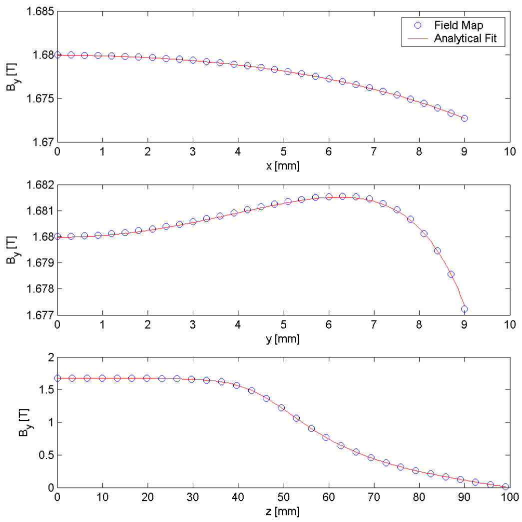

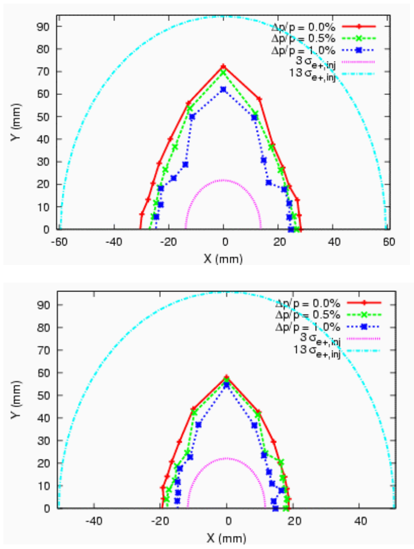

Far left: field strength variations in a model of the TESLA hybrid wiggler.

Left: Dynamic aperture in an ILC damping ring with linear (top) and nonlinear (bottom) wiggler models.

Vacuum system

The vacuum system must:

- provide the very low (< 1 ntorr) vacuum pressure needed to avoid electron cloud and ion effects;
- handle safely the intense synchrotron radiation from the damping wigglers and dipoles;
- implement measures to avoid build-up of electron cloud;
- have low impedance for classical multi-bunch and single-bunch instabilities;
- have a design consistent with the magnet systems, and with the operational performance specifications for the instrumentation and diagnostics.

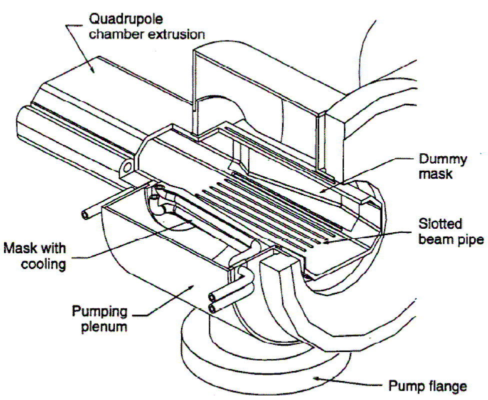

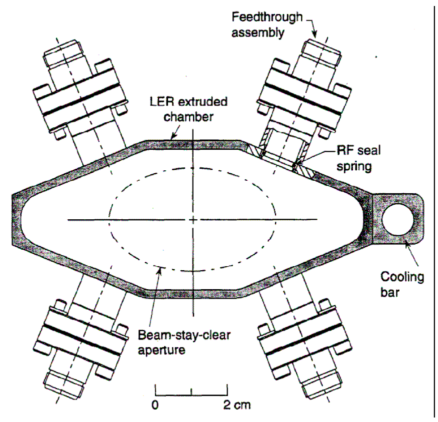

Vacuum chamber components from PEP-II (SLAC-R-418)

Electron cloud effects

In a positron (or proton) storage ring, electrons are generated by a variety of processes, and can be accelerated by the beam to hit the vacuum chamber with sufficient energy to generate multiple "secondary" electrons.

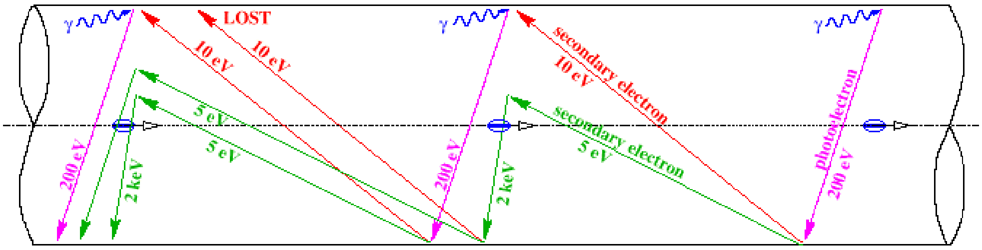

Under the right conditions, the density of electrons in the chamber can reach high levels, and can drive instabilities in the beam.

Important parameters determining the electron cloud density include:

- the bunch charge and bunch spacing;
- the geometry of the vacuum chamber;
- the properties of the vacuum chamber surface (the "secondary electron yield").

The secondary electron yield (SEY) of a surface is a key parameter

The secondary electron yield specifies the number of electrons emitted from a surface per primary incident electron.

The number of secondary electrons emitted in any particular event depends on the energy and angle of incidence of the primary electron, as well as the properties of the surface.

Surfaces of nominally the same material can show very different properties, depending on the history of the material.

For convenience, we often quote a single number for the SEY, which gives the maximum number of electrons emitted per incident electron under any conditions.

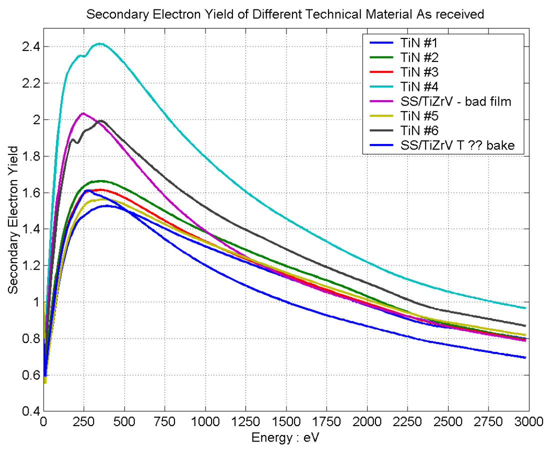

From Bob Kirby and Frederic le Pimpec.

Determining the density of the electron cloud in an accelerator

The development of an electron cloud in an accelerator environment is a complicated process, depending on details of the beam distribution and on the chamber geometry and surface properties.

Significant effort has been devoted to developing accurate computer simulations of the build-up process, which allow specification of:

- beam charge and time structure;
- chamber geometry (including antechamber);
- chamber surface properties;
- various sources of electrons (including secondary emission, photoelectrons, gas ionisation);
- properties of secondary electrons (energy and angular distribution);
- external electromagnetic fields.

Codes are available that make detailed simulations of the electron-cloud build-up and dynamics, including such effects as the space-charge of the cloud itself.

The output of the simulation codes includes the density distribution of the cloud in the vacuum chamber, and its time evolution.

Determining the density of the electron cloud in an accelerator

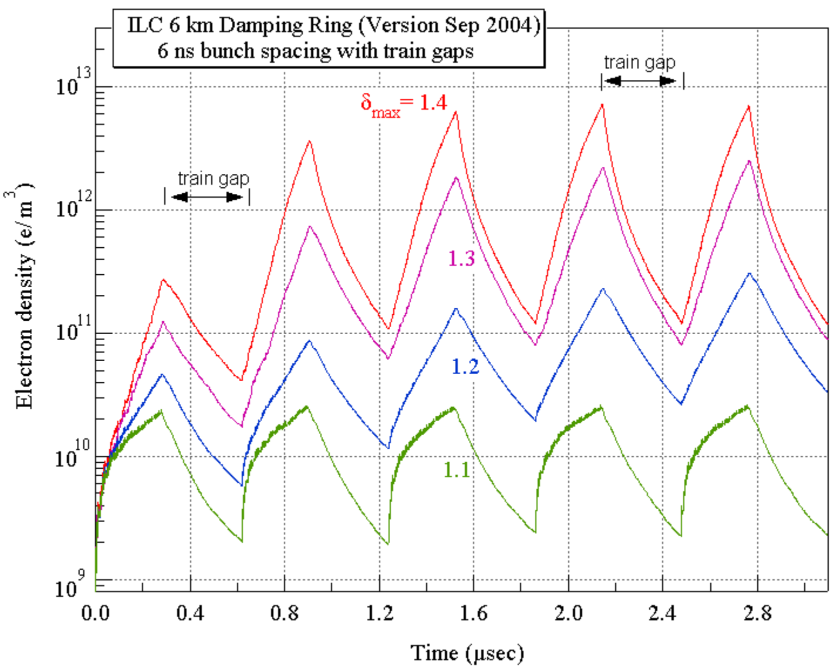

Posinst simulation of average electron cloud density in a drift space in a 6 km design for the ILC positron damping ring, by Mauro Pivi.

The electron cloud density can reach the neutralisation density

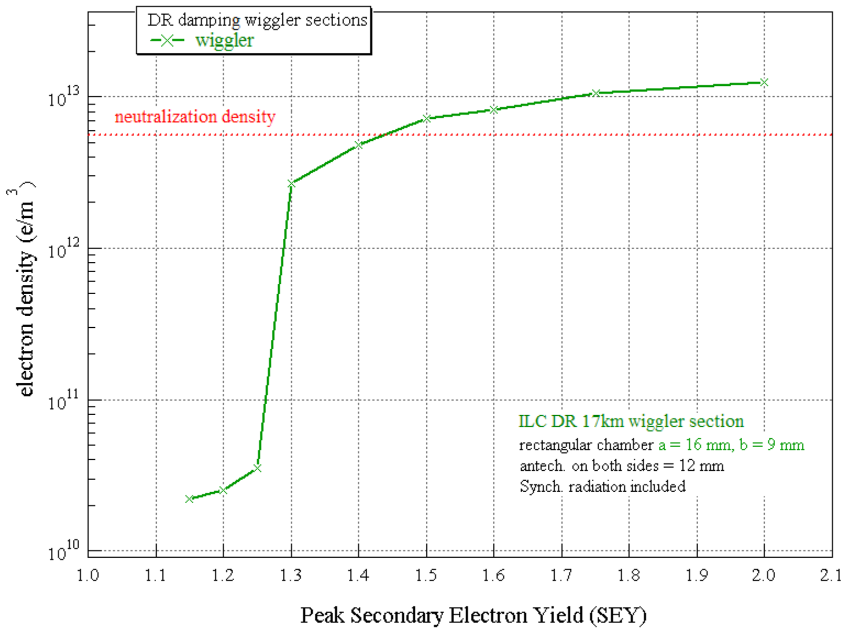

The neutralisation density is the point where there are as many electrons inside the vacuum chamber as there are positrons.

External magnetic fields can "trap" low-energy electrons

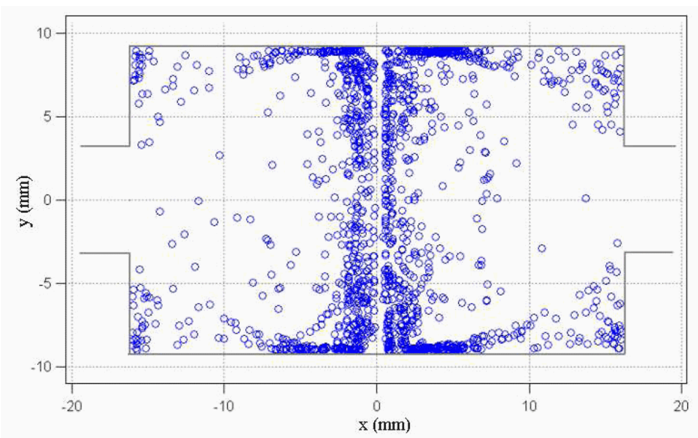

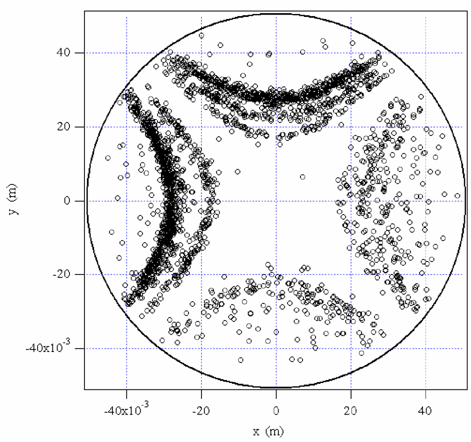

Simulations of electron cloud in the wiggler of the TESLA damping ring (left), and in a quadrupole in the PSR (right), by Mauro Pivi.

Observations of electron cloud: increase in residual gas pressure

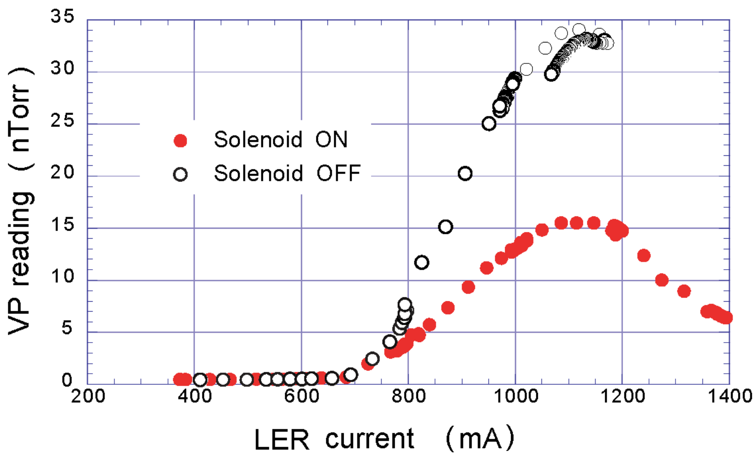

Observations of pressure rise in the PEP II LER.
A. Kuliokov et al, Proceedings of PAC01.

Observations of electron cloud: tune shifts

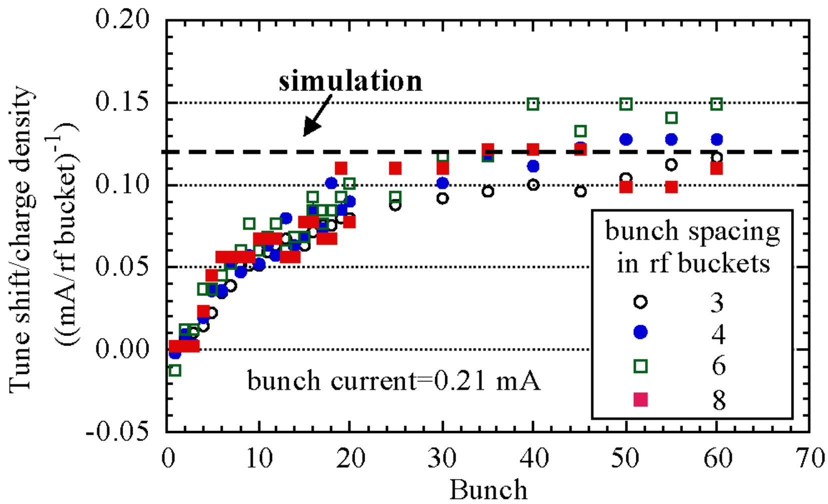

Measurements of vertical tune shift as a function of bunch number in a bunch train in KEKB.
H. Fukuma, Proceedings of ECLOUD02.

Observations of electron cloud: increase in beam size

solenoids off

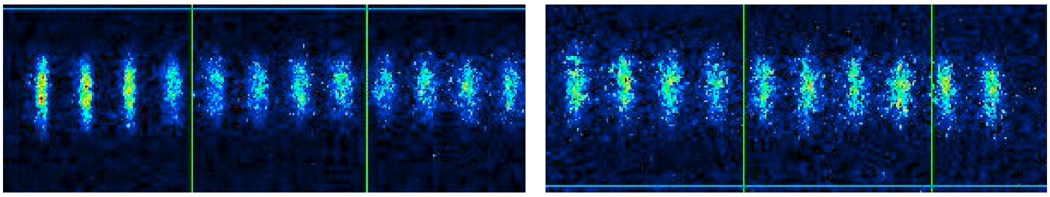

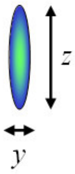

head of bunch train tail of bunch train

solenoids on

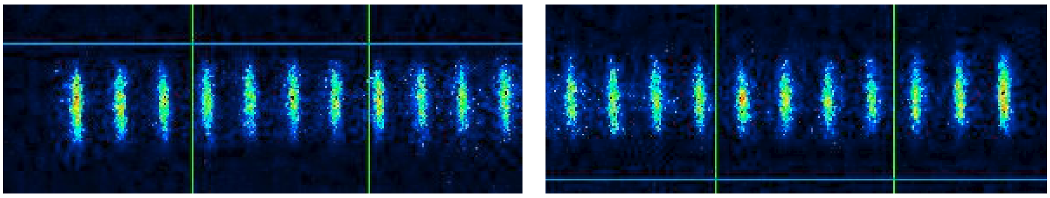

head of bunch train tail of bunch train

Observations of beam-size increase in KEKB.
H. Fukuma, Proceedings of ECLOUD04.

Suppressing the build-up of electron cloud

Electron cloud could limit the operational performance of the damping rings.

Without implementing some measures to suppress the build-up of electron cloud, we expect that the cloud density will approach the neutralisation density, and that beam instabilities will occur.

There are a number of techniques that can be used to suppress the build-up of electron cloud in an accelerator.

- Adjusting the beam parameters.

  Higher energy, lower current, larger momentum compaction all help to reduce the rate of build-up of electron cloud or mitigate its impact on the beam. Actions in this category may be difficult to implement after construction.

- Treating or conditioning the vacuum chamber surface.

  The chamber surface can be coated with a material having low SEY.

  Grooves can be cut into the chamber surface.

- Applying external fields.

  Solenoids trap electrons near the wall of the vacuum chamber.

  Clearing electrodes can similarly prevent build-up of electron cloud in the vicinity of the beam.

Suppressing electron cloud with low-SEY coatings

Coatings that have been investigated include TiN and TiZrV.

Achieving a peak SEY below 1.2 seems possible after *conditioning*.

Reliability/reproducibility and durability are concerns.

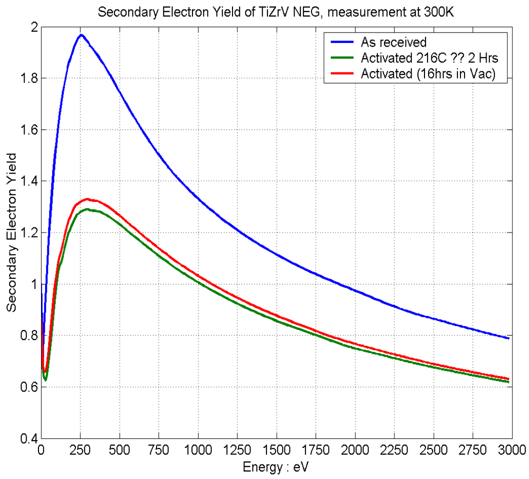

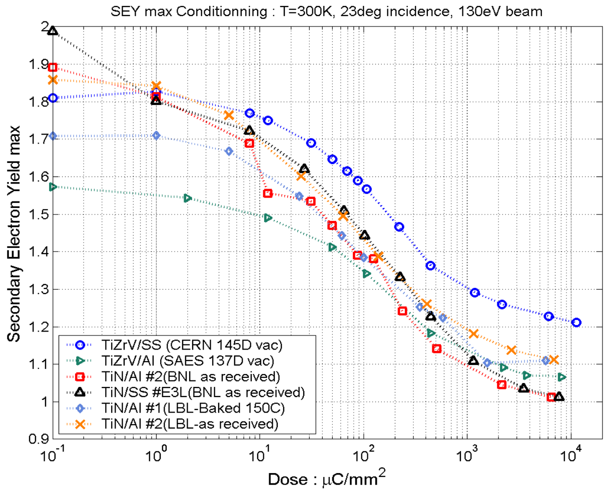

Measurements of SEY of TiZrV (NEG) coating. (F. le Pimpec, M. Pivi, R. Kirby)

Suppressing electron cloud with a grooved vacuum chamber

Electrons entering the grooves release secondaries which are reabsorbed at low energy (and hence without releasing further secondaries) before they can be accelerated in the vicinity of the beam.

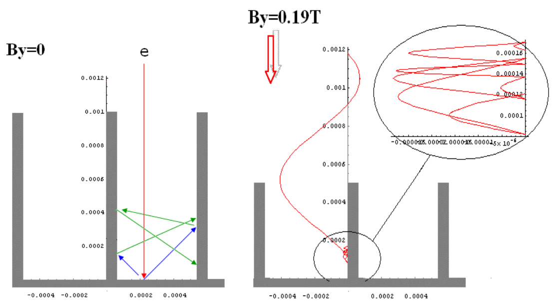

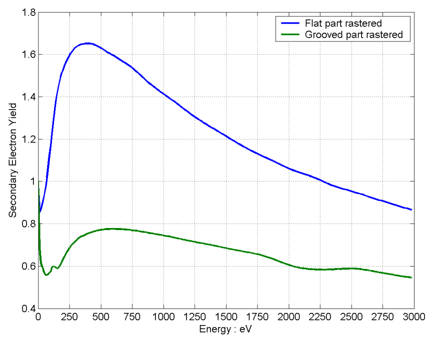

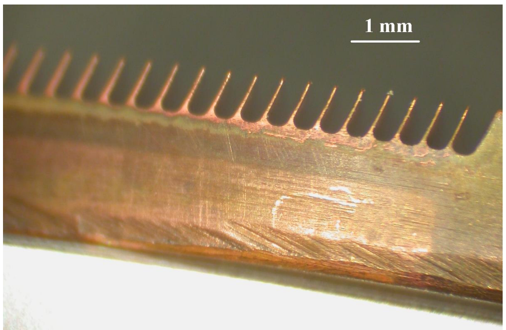

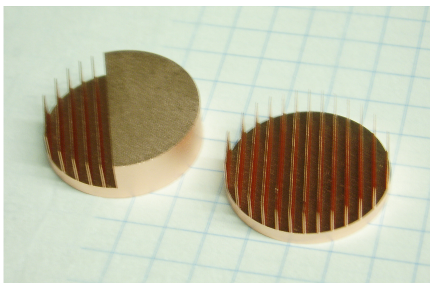

Suppressing electron cloud with solenoids

A solenoid field keeps secondary electrons close to the wall, where they can be re-absorbed without gaining enough energy to release further secondaries. However, there is evidence for a "resonance" effect, which occurs when the field strength leads to a time of flight for the electrons equal to the bunch spacing.

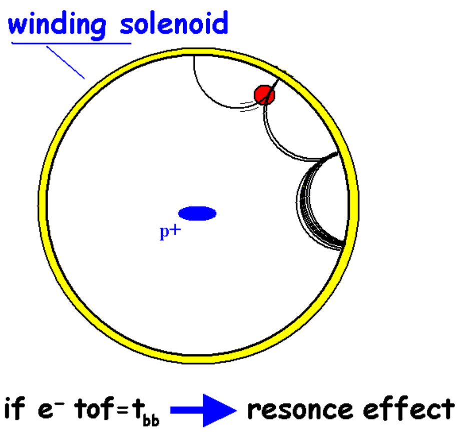

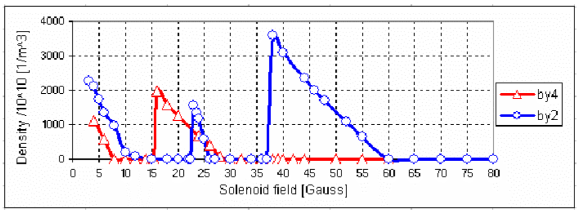

e⁻ density at by-2 and 4 RF buckets spacing in PEP II LER.
A. Novokhatski and J. Seeman (PAC03)

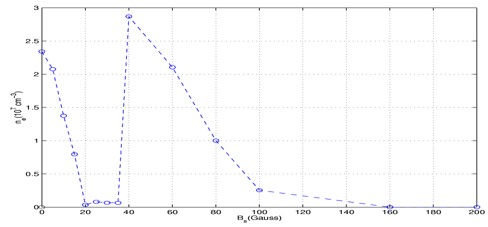

e⁻ density at by-2 RF buckets spacing in PEP II LER.
Y. Cai and M. Pivi (PAC03)

Suppressing electron cloud with clearing electrodes

Low-energy secondary electrons emitted from the electrode surface are prevented from reaching the beam by the electric field at the surface of the electrode. This also appears to be an effective technique for suppressing build-up of electron cloud.

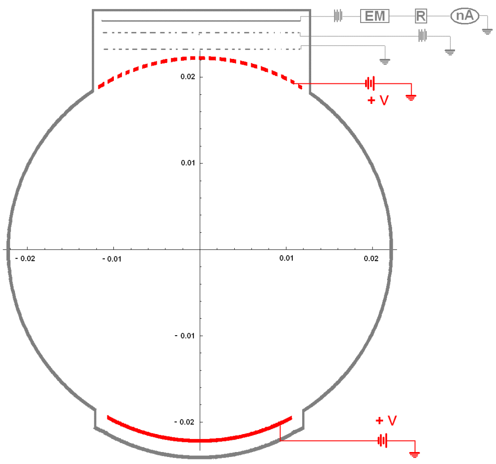

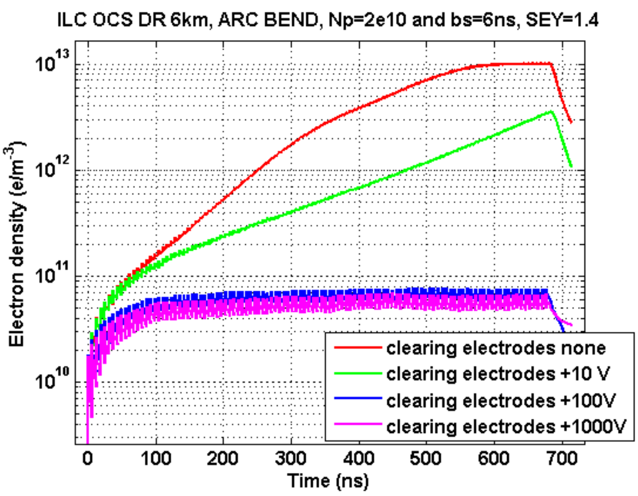

Ion effects

While electron cloud effects are a concern for the positron rings, ion effects are a concern for the electron rings.

In electron storage rings, residual gas molecules can be ionised by the beam. The resulting positive ions may then be trapped in the electric field of the beam, and accumulate to high density. The fields of the ions can then drive beam instabilities.

The differences between electron cloud and ion effects arise principally from the difference in mass between electrons and ions. While electrons move rapidly on the time scale of a single bunch passage, ions move relatively slowly. The dynamical behaviour is then somewhat different.

If a storage ring is uniformly filled with electron bunches, then ions accumulate over many turns. This leads to the well-known phenomenon of ion trapping, which is usually solved by including one or more "gaps" in the fill pattern.

However, under certain conditions, sufficient ions can accumulate in the passage of a small number of bunches to drive an instability, known in this case as the "fast ion instability".

Ion trapping

Consider an ion of relative molecular mass A moving in the electric fields of a sequence of electron bunches:

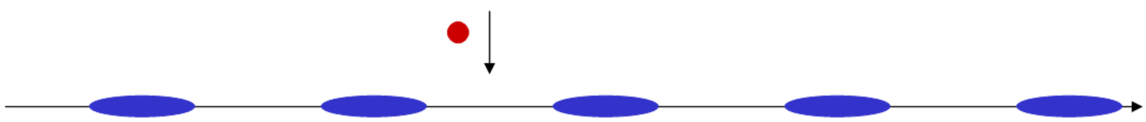

Making a linear approximation to the electric field around a bunch, the kick given to the ion as the bunch goes past can be represented by a focusing force k:

$$k = \frac{2r_p N_0}{A\sigma_y(\sigma_x + \sigma_y)}$$

where r_p is the classical radius of the proton, N_0 is the number of electrons in a bunch, and σ_x and σ_y are the rms bunch sizes.

Ion trapping

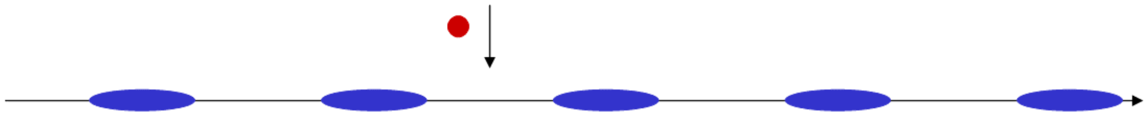

The motion of the ion over a period represented by one bunch and the following gap before the next bunch arrives, can be represented by a transfer matrix:

$$\begin{pmatrix} 1 & s_b \\ 0 & 1 \end{pmatrix} \cdot \begin{pmatrix} 1 & 0 \\ -k & 1 \end{pmatrix} = \begin{pmatrix} 1 - s_b k & sb \\ -k & 1 \end{pmatrix}$$

As we know from linear beam dynamics, the motion is only stable if the absolute value of the trace of the periodic transfer matrix is less than 2. Hence, for the motion of the ion to be stable, we require:

$$0 < s_b k < 4$$

which means that:

$$A > \frac{r_p N_0 s_b}{2\sigma_y (\sigma_x + \sigma_y)}$$

Ion trapping

The ion trapping condition is:

$$A > \frac{r_p N_0 s_b}{2\sigma_y (\sigma_x + \sigma_y)}$$

This tells us that for large bunch charges, or bunches with very small transverse dimensions, only very heavy ions will be trapped.

In the damping rings, the beam sizes are large at injection, and all ions can be trapped. But during damping, the beam sizes decrease and the minimum mass of trapped ions steadily increases.

We can compare the minimum mass of trapped ions in the ILC damping rings at injection and at equilibrium, assuming normalised injected emittances of 45 μm:

	Injection	Equilibrium
N_0	2×10^{10}	2×10^{10}
s_b	1.8 m	1.8 m
σ_x	600 μm	250 μm
σ_y	300 μm	6 μm
A_{min}	0.10	18

Fast ion instability

We can prevent multi-turn ion trapping by including gaps in the fill, i.e. by periodically having a very large separation between two bunches (ten or twenty times larger than normal).

However, ions accumulating during the passage of a small number of bunches can still drive instabilities.

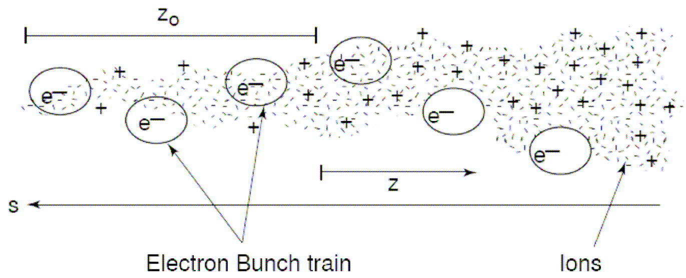

The theory of "fast ion instability" has been developed by Raubenheimer and Zimmermann:

T. Raubenheimer and F. Zimmermann, Phys. Rev. E **52**, 5, 5487 (1995).

Fast ion instability

The fast ion instability can be treated as a coupled-bunch instability, with a growth rate $1/\tau_e$ given by:

$$\frac{1}{\tau_e} \approx \frac{1}{3}\sqrt{\frac{2}{3}}\frac{c}{\Delta\omega_i/\omega_i}\beta_y k_y$$

where k_y is the focusing force on the beam from the ions, β_y is the beta function, and $\Delta\omega_i/\omega_i$ is the relative spread of oscillation frequencies of ions in the beam. Normally, we can assume that:

$$\Delta\omega_i/\omega_i \approx 0.3$$

The focusing force of ions on the beam is given by:

$$k_y = \frac{\lambda_i r_e}{\gamma\sigma_y(\sigma_x + \sigma_y)}$$

where we assume that the transverse distribution of the ions is comparable to that of the particles in the beam, and the longitudinal ion density is:

$$\lambda_i = \sigma_i \frac{p}{kT} N_0 n_b$$

The longitudinal ion density depends on the ionisation cross section σ_i, on the residual gas pressure p, on the number of particles in each electron bunch N_0 and on the number of bunches n_b that have passed.

Observation of fast ion instability in the LBNL-ALS

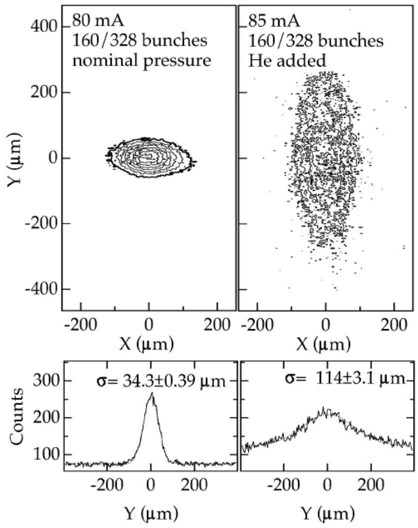

FIG. 1. Transverse profile images (shown as contour plots) of the beam for nominal pressure and with He added; the vertical profile for each image is also shown, along with a fit to a Gaussian distribution.

J. Byrd et al, "First observations of a fast beam-ion instability", Phys. Rev. Lett. **79**, 79-82 (1997).

Observation of fast ion instability in the LBNL-ALS

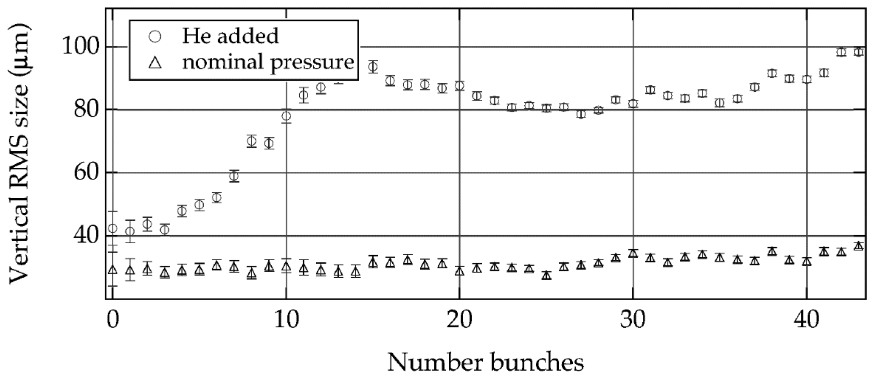

FIG. 2. rms vertical beam size vs the number of bunches for nominal and elevated pressure conditions.

J. Byrd et al, "First observations of a fast beam-ion instability", Phys. Rev. Lett. **79**, 79-82 (1997).

Measurements of fast ion instability in KEK-ATF

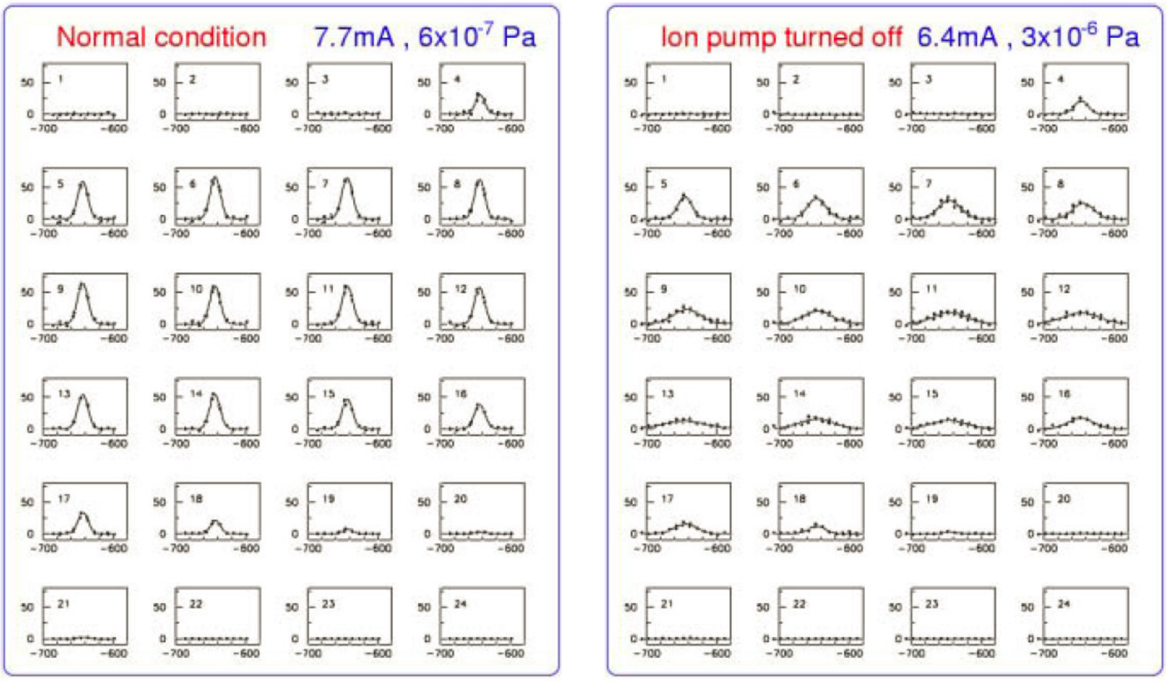

Bunch profile measurements made using laser wire in ATF damping ring, by Yosuke Honda (presented at ISG XI, KEK, 2003).

Measurements of fast ion instability in KEK-ATF

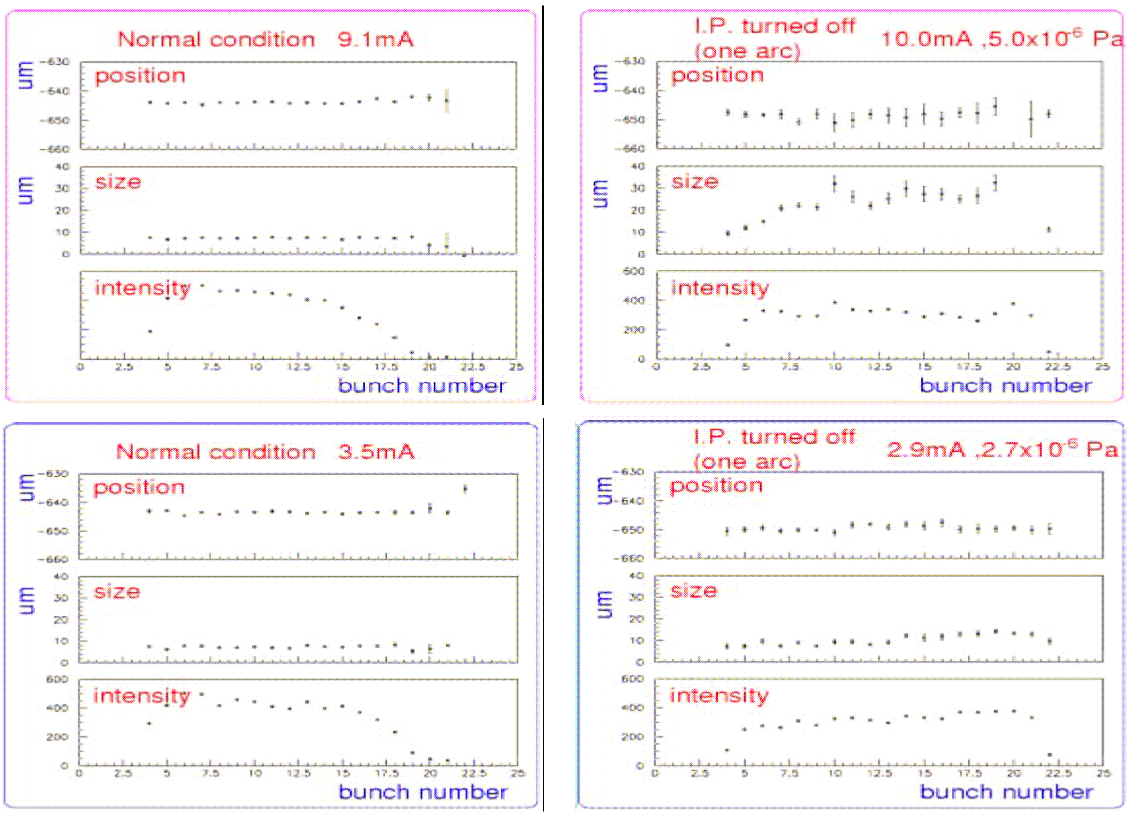

Fast ion instability in the ILC damping rings

Simulations suggest that the growth rates might be somewhat slower than suggested by the analytical formulae. Also, there is some evidence that the effects of the ions are mitigated by decoherence of the ions, and that the effect may saturate at low levels.

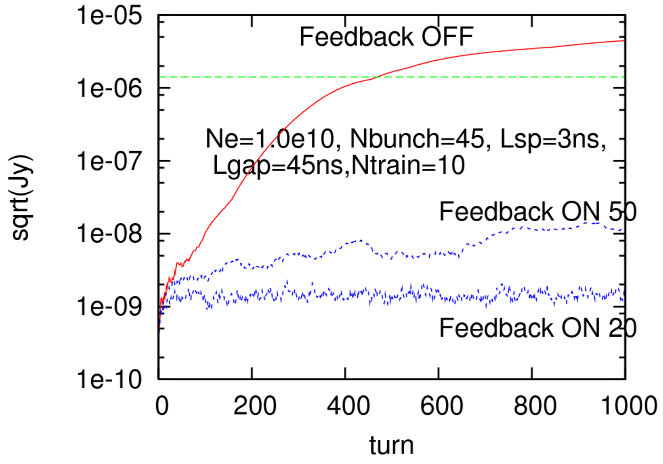

Simulation of fast ion instability in a recent 6.7 km lattice for the ILC damping rings, by Kazuhito Ohmi.

Studies are ongoing to develop a reliable model for the ion effects in the damping rings. At present, it is regarded as prudent to specify the vacuum system to achieve quite demanding residual gas pressures.

Summary of electron cloud and ion effects

Electron cloud is one of the main concerns for the ILC damping rings. Studies suggest that without taking preventative measures, electron cloud in the positron damping ring could reach densities (close to the neutralisation density) sufficient to drive instabilities in the positron beam.

Some simple analytical models can be used to describe the dynamics of a positron beam with electron cloud; but more reliable estimates can be obtained using simulation codes.

A variety of methods for suppressing the build-up of electron cloud are available, and some look promising for the ILC damping rings. Research and development are ongoing to develop a sufficiently effective means of suppressing build-up of electron cloud in the damping rings.

Ion effects are a concern for the electron damping ring. Instability growth rates for the fast ion instability appear fast when estimated from simple analytical formulae. However, more detailed simulations suggest that the effects may be less severe, and could be mitigated using bunch-by-bunch feedback systems.

Studies of ion effects are continuing.

Instrumentation and diagnostics

The demanding specifications for beam quality and stability in linear collider damping rings will only be achieved with high-performance instrumentation and diagnostics.

Key devices include:

- beam position monitors (BPMs) with micron-resolution turn-by-turn capability, and excellent stability;
- fast beam size monitors, capable of beam size measurements with resolution < 10 microns, on time scales of milliseconds;
- a variety of devices for characterising and diagnosing a range of beam instabilities.

Fast x-ray synchrotron radiation beam size monitor

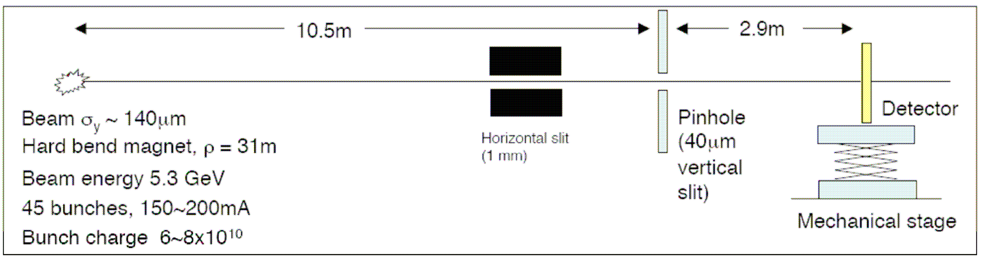

Prototype tested in CHESS (2006)

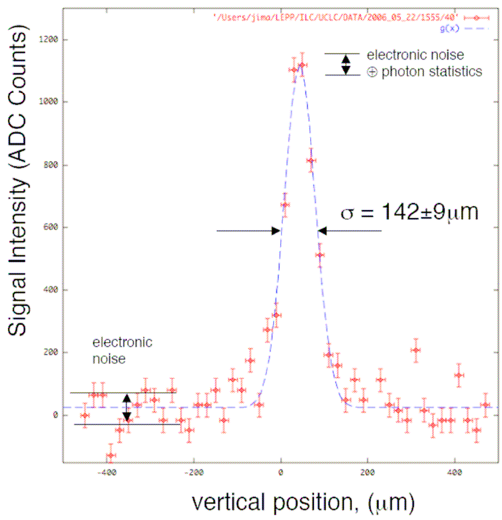

Courtesy of Jim Alexander (Cornell)

Fast x-ray synchrotron radiation beam size monitor

Next prototype: October 2007

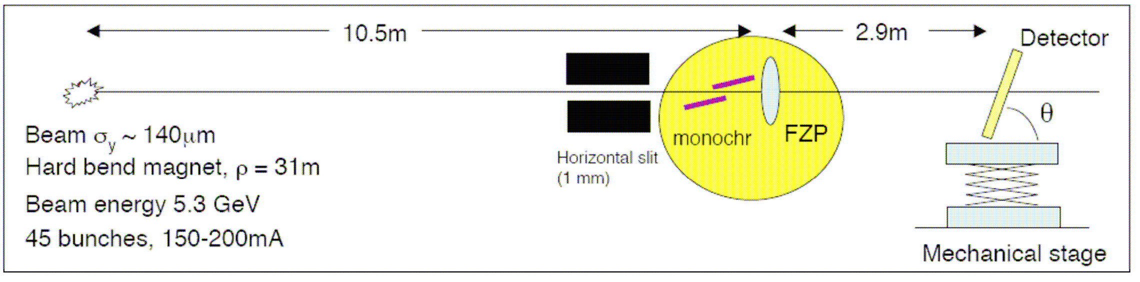

Next prototype will test all key components of CesrTA design:

- multilayer mirrors, cooling, mechanics, alignment, orientation
- Fresnel Zone Plate .. x3 demagnification (okay - large beam)
- full size 1-dim detector, 32++ channels simultaneous readout
- test adjustable effective pixel height ($\Delta x \sin\theta$)
- single pass, single bunch snapshot imaging, as before
- improved high BW, low noise readout
- study radiation damage in more detail than previous run

Laser wire beam size monitor: demonstrated in KEK-ATF

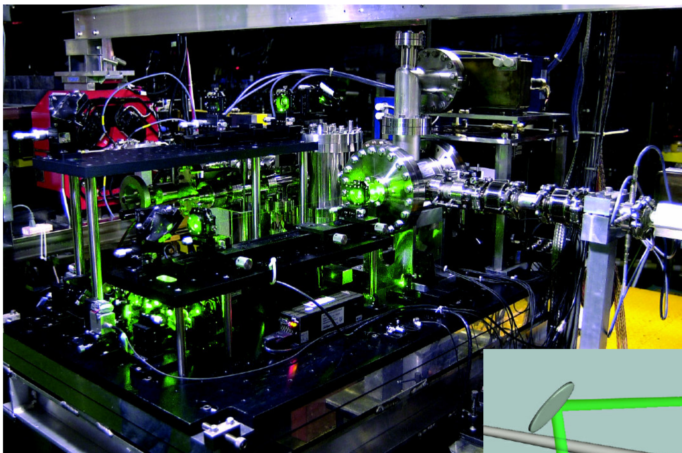

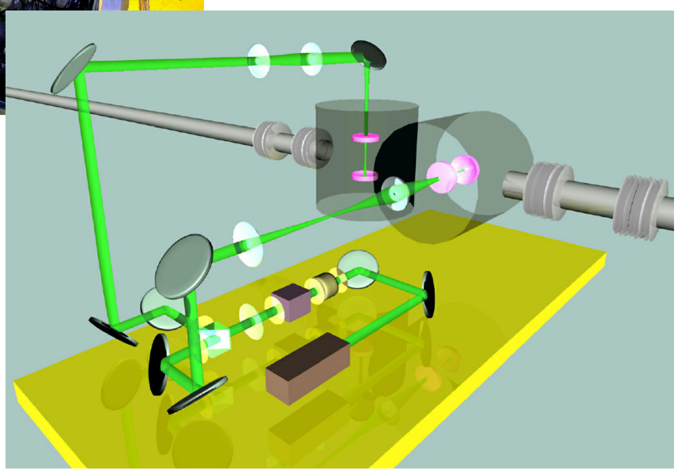

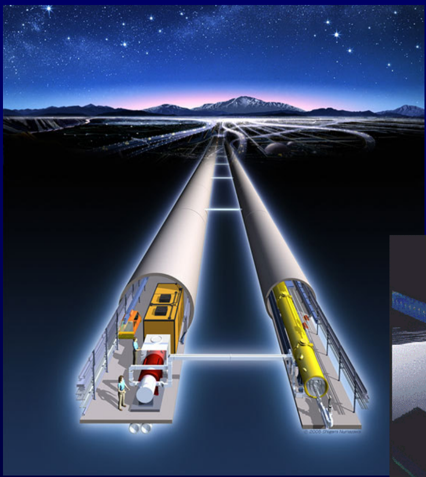

The damping rings will play a critical role in **generating luminosity** in the ILC. A wide range of accelerator physics and technology issues need to be addressed if the damping rings are to meet their performance specifications.

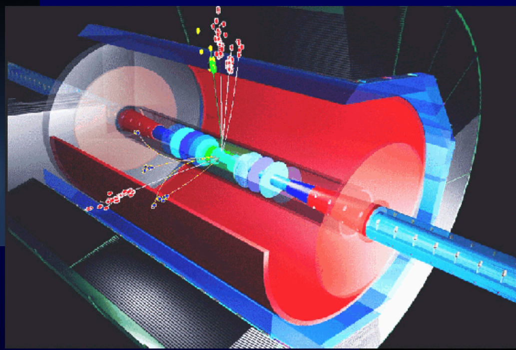

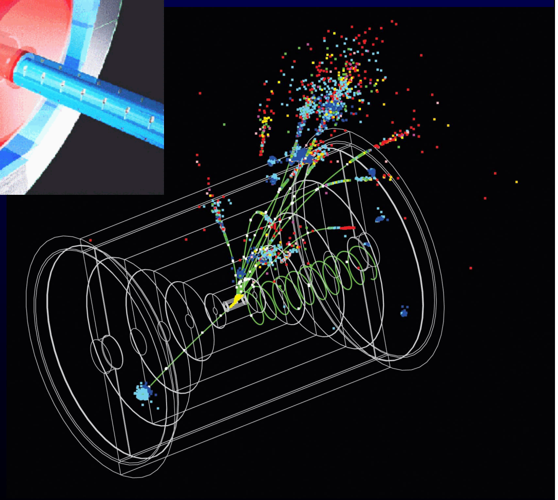

Thank you for your attention!